INSTITUTE OF PHYSICS PUBLISHING SMART MATERIALS AND STRUCTURES
Smart Mater. Struct. **16** (2007) 106–113 doi:10.1088/0964-1726/16/1/013

Adaptive energy-absorbing materials using field-responsive fluid-impregnated cellular solids

Suraj S Deshmukh and Gareth H McKinley

Hatsopoulos Microfluids Laboratory, Department of Mechanical Engineering and Institute of Soldier Nanotechnologies (ISN), Massachusetts Institute of Technology, Cambridge, MA 02139, USA

E-mail: gareth@mit.edu

Received 21 April 2005, in final form 26 September 2006
Published 6 December 2006
Online at stacks.iop.org/SMS/16/106

Abstract
Adaptive materials with rapidly controllable and switchable energy-absorption and stiffness properties have a number of potential applications. We have developed, characterized and modeled a class of adaptive energy-absorbing systems consisting of nonlinear poroelastic composites wherein a field-responsive fluid, such as a magnetorheological fluid or a shear-thickening fluid, has been used to modulate the mechanical properties of a cellular solid. The mechanical properties and energy-absorbing capabilities of the composite are studied for variations in design parameters including imposed field strength, volume fraction of the field-responsive fluid within the composite and impact strain rates. The total energy absorbed by these materials can be modulated by a factor of 1- to 50-fold for small volume fractions of the fluid (∼15%) using moderate magnetic fields varying from 0 to 0.2 T. A scaling model is also proposed for the fluid–solid composite mechanical behavior that collapses experimental data onto a single master curve. The model allows optimization of the composite properties in tune with the application requirements. Potential application areas are discussed with emphasis on applicability in impact-absorbing headrests and cushioned assemblies for energy management.

(Some figures in this article are in colour only in the electronic version)

M This article features online multimedia enhancements

1. Introduction

Energy-absorbing materials and structures are used in a number of applications ranging from vehicles, ballistic armor, blast protection to helmets, sporting equipment and clothing [1, 2]. Such materials will shunt (divert and distribute energy to sturdier areas), convert or dissipate energy via viscosity, friction, viscoelasticity or plasticity [3, 4]. However, passive systems like cellular solids, foams, sandwich structures, etc, are typically used, which, although effective under certain predefined scenarios, provide little to no utility under a different set of conditions. Many of these applications, on the other hand, require an adaptive structure that can be controlled to absorb varying amounts of energy depending on the external conditions [5–8]. A representative application area is the automotive industry where adaptive energy-absorbing materials could prove beneficial in overcoming the energy management concerns in occupant protection components for passenger and vehicle safety. A compliant material forming these parts generates low forces and is comfortable but absorbs very little energy, while thicker, stiffer materials will absorb more energy but conflict with design and passenger demands

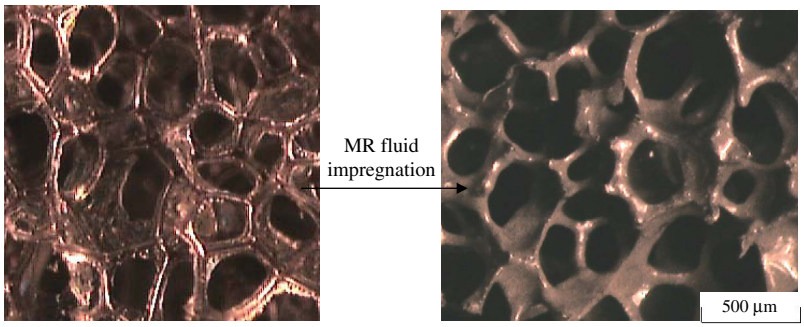

Figure 1. Optical micrograph (*Olympus SZX9 microscope*) of a dry low-density reticulated foam after impregnation with a commercially available MR fluid (*LORD's MRF-336AG*).

for slim, narrow structures. Hence, there is a trade-off in the optimal stiffness property of the selected materials and an adaptive material is necessary to resolve this conflict. This is commonly referred to as the *conflict of stiffness* problem [5, 7].

This paper describes the development and mechanical characterization of such a *'smart'* (responsive to external conditions or user-controllable) energy-absorbing material. It is a fluid–solid composite consisting of an elastomeric foam impregnated with a field-responsive fluid (FRF) such as a magnetorheological fluid (MRF) or a shear-thickening fluid (STF).

A field-responsive fluid may be characterized as a material that undergoes large changes in its rheological (i.e. flow) properties in response to changes in magnetic, electric or stress fields [9–12]. Many applications utilize their variable flow rate or force characteristics in either damping or torque transfer scenarios and proposed applications include shock absorbers, clutches, brakes, actuators and artificial joints. In this paper these large reversible changes in fluid properties are used to modulate the energy absorption capacity and mechanical properties of cellular solids.

Magnetorheological fluids ('MR fluids') belong to the broad class of field-responsive fluids and are 20–50% v/v suspensions of magnetizable particles, usually 1–10 μm in diameter, in a carrier fluid such as mineral oil, silicone oil or water [11]. Normally, MR fluids are in the liquid state with a viscosity ∼0.1–1 Pa s but when a magnetic field is applied, the soft magnetic particles acquire a dipole moment and align with the external field relative to the non-magnetized dispersed phase to form fibrous columns or aggregates [12]. These columns must be deformed and broken for the suspension to flow, giving rise to a yield stress [13] that is a function of the magnetic flux density. Many earlier studies have focused on determining this yield stress and other rheological properties of MR fluids under steady shear and oscillatory shear flow [14, 15].

2. Concept and development of the adaptive material

A cellular solid [1], a porous interconnected network of solid material forming edges and faces of cells, such as an open-cell or reticulated foam, is impregnated with a field-responsive fluid, such as a magnetorheological fluid, to result in an *adaptive fluid–solid composite*. The stiffness and the energy-absorbing properties of this composite can be varied by controlling and adjusting the field strength in the vicinity of the material.

The method of impregnation of the MR fluid inside the reticulated foam pores is by suction, i.e. the cellular solid is compressed at a constant rate by a mechanical compression device, while being immersed in a measured amount of MR fluid and is then allowed to relax which causes the fluid to fill up the pores. Repeated compression and relaxation then results in spatial homogenization of the MR fluid inside the pores of the reticulated foam. The fluid forms a secondary layer covering the solid struts of the cellular solid where it is held in place owing to its finite off-state yield stress (τ_y^0), as shown in figure 1. The thickness of this secondary layer is found to be of the order of $h \sim \tau_y^0/\rho g$, where $\rho \simeq 3.45$ g cm^{-3} is the density of the MR fluid.

The cellular solid with its absorptive matrix is able to effectively hold the MR fluid in place which also reduces sedimentation problems that are typically encountered in MR fluid based damper applications. Carlson's group [16, 17] use this elegant and cost-effective method of holding MR fluid in place in washing machine dampers and other vibration control devices. However, in this earlier work, the foam matrix phase acts primarily as a passive fluid support between two moving members of the damper and the structure is sheared orthogonal to the applied field. We exploit the compressive properties of the elastomeric foam and utilize the field-dependent MR fluid behavior to actively vary the modulus in compression and to control the energy absorption capacity of the fluid–solid composite.

We also synthesize an inexpensive stable magnetorheological fluid in-house [15], which can then be impregnated into a cellular solid. The changes in rheological properties of the field-responsive fluid as a function of the applied field determine the adaptive mechanical properties of the energy-absorbing material. Hence, rheological measurements in steady and transient shear flows are performed using a parallel plate rheometer (TA Instruments' AR 2000) together with a custom-fabricated fixture that generates a homogeneous magnetic field. In figure 2 we compare the yield-stress data extracted for the synthesized fluid with other commercially available MR fluids [18]. The subquadratic variation in the plastic yield stress as a function of the externally imposed magnetic field strength enables us to evaluate the energy absorption capacity of the fluid-impregnated composite. Additional rheological details such as the viscoelastic properties and the response time of the fluid are supplied elsewhere [15].

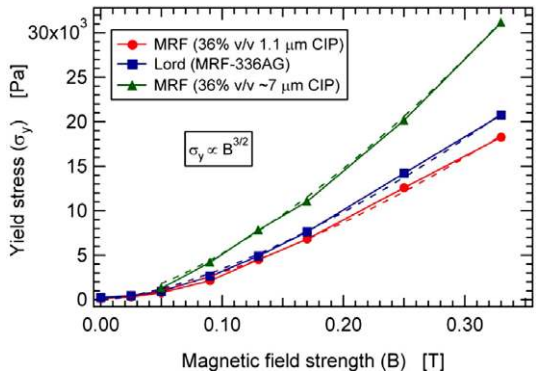

Figure 2. Yield-stress comparison for three MR fluids, one commercially available and two synthesized in our laboratory. The dotted lines show the subquadratic dependence ($\sigma_y \propto B^{1.5}$) of yield stress on the magnetic field strength.

3. Mechanical properties: stress–strain behavior and energy-absorption capacities of MRF impregnated cellular solids

3.1. Experimental set-up

The stress–strain and energy absorption behavior of these fluid–solid composites is determined using the Texture Analyzer (TA.XT2i), a programmable strain-rate ($10^{-8} \leqslant \dot{\varepsilon} \leqslant 10^{-2}$ s^{-1}) testing instrument. A fixture for the texture analyzer was designed so that the foam is confined in a piston–cylinder type arrangement to prevent spontaneous deformation of the material on application of a high magnetic field gradient and to ensure unidirectional fluid flow along the direction of compression. The texture analyzer controls a piston-type compression probe and executes constant velocity or constant strain-rate compression protocols, while measuring accurately the force, displacement and other dynamic quantities.

Open-cell reticulated polyurethane foam with solid elastic modulus (E_s) = 45 MPa, density of solid (ρ_s) = 1200 kg m^{-3}, relative density (ρ^*/ρ_s) = 0.0155 and comprising of tetrakaidecahedron cells of ∼300 μm pore size is used in all experiments. A horseshoe type permanent magnet provides the desired magnetic field and can be moved along the vertical direction to obtain various magnetic field gradient profiles along the direction of deformation. A gaussmeter (F. W. Bell Model 5060) with an axial and transverse probe and a resolution of 1 mT (10 G) is used to measure the applied magnetic field and its variation with sample height. All the experiments are performed when a high magnetic field gradient is imposed on the foam sample and only the average magnetic field strength is indicated in the plots.

3.2. Experimental results and discussion: stress–strain behavior

A secondary layer of MR fluid is formed on the cell struts upon impregnation and hence magnetic field strength becomes the important user-controllable parameter. The magnetic field strength determines the yield stress of the MRF, which in turn controls the plateau modulus of the composite material, here denoted σ^*, and also its ultimate energy absorption capacity.

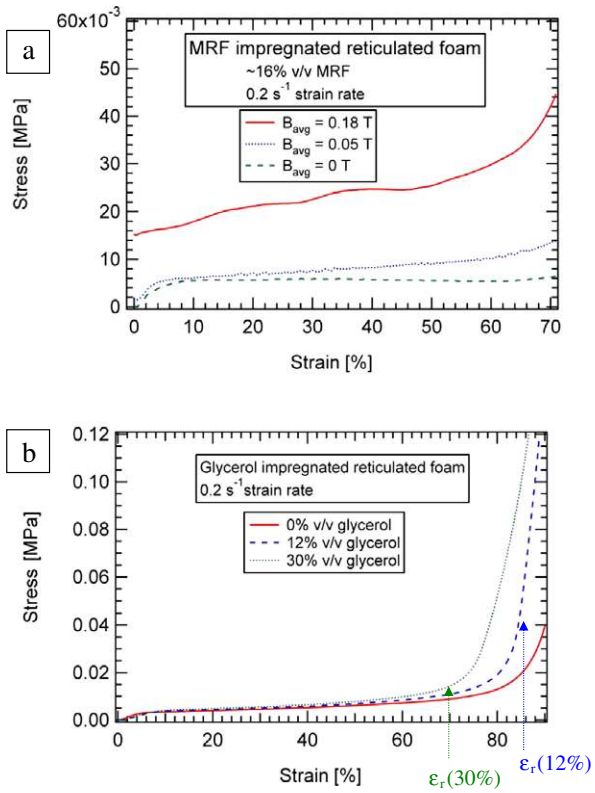

Figure 3. (a) Stress–strain curves for MR fluid impregnated open-cell foam (16% v/v) at different magnetic field strengths. (b) Characteristic stress–strain curves for glycerol-filled reticulated foams at varying volume fractions of the fluid at low strain rates.

Hence, as the magnetic field is increased to moderate levels of $B_{avg} \sim 0.2$ T, while keeping other parameters constant, the yield stress of the MR fluid increases and correspondingly an upward shift in the plateau stress is observed. This jump, which is quite dramatic at higher magnetic fields, is shown and compared with the stress–strain behavior observed at lower and zero magnetic fields in figure 3(a).

We can also compare this stress–strain response with that obtained when cellular solids are impregnated with fluids that are not field-responsive, e.g. Newtonian fluids such as glycerol. In this case the plateau modulus (σ^*) changes by less than 15% though a shift in the densification strain is observed, as illustrated in figure 3(b). The reduced densification strain (ε_r) for fluid-impregnated foams can be estimated as a function of the volume fraction of the impregnating fluid to be

$$\varepsilon_r \approx \varepsilon_D (1 - \phi_f) \tag{1}$$

where ε_D is the densification strain for a 'dry' foam which is derived from classical foam theory [1] and ϕ_f is the fluid volume fraction. This scaling is based on the expression for free volume that determines the densification strain when the opposing cell walls are crushed together and the incompressibility of the solid and liquid phases is observed.

The marked difference in the effective composite mechanical properties shown in figures 3(a) and (b) occurs principally for the following reason; for foams filled with a viscous Newtonian fluid only the volume of the displaced fluid

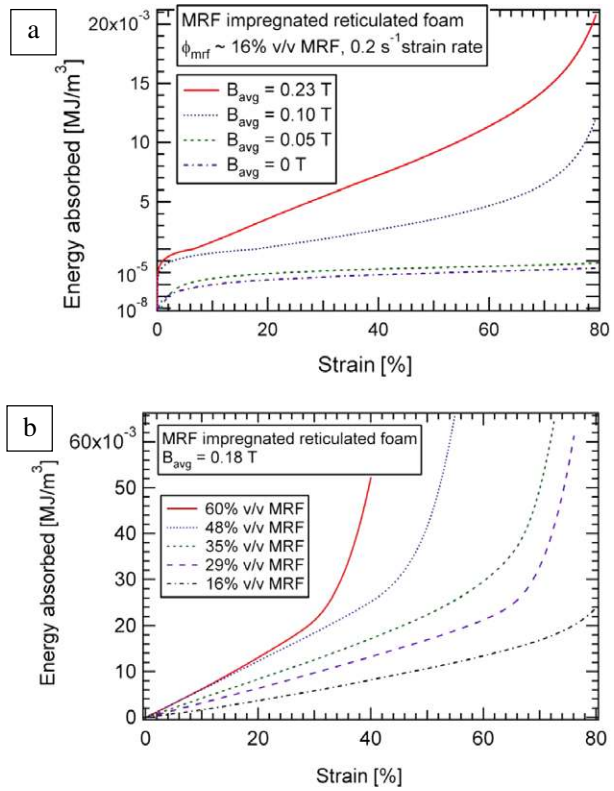

Figure 4. (a) Variation of energy absorption capacity by modulating the magnetic field strength for 16% v/v MR fluid-filled open-cell foam. (b) Energy absorption curves for MR fluid-impregnated foam at 0.18 T (average) depicting increase in the plateau stress (σ^*) and energy absorption along with shift in the densification region as the volume fraction of the fluid is varied from 15% to 60%.

changes, whereas in the case of MR fluid-impregnated foams, not only does the apparent viscosity of the displaced fluid increase due to the large yield stress but also the fluid-coated struts forming the cell edges are mechanically reinforced. Thus, as a result of this field-dependent yield stress the effective plateau modulus of the composite itself is increased.

3.3. Experimental results and discussion: energy absorption capacity

The energy absorbed per unit volume or the *energy absorption capacity* can be obtained as the area enclosed by the stress–strain curve for the material. From the stress–strain behavior of MR fluid-impregnated foams it can be inferred that the energy absorbed increases significantly even at moderate magnetic fields and low volume fractions of the fluid. Further it can be increased by a factor of 30–50 times the energy absorbed at zero field as shown in figure 4(a). The figure is shown partially in a logarithmic scale and partially in a linear scale in order to illustrate the low amounts of energy absorbed in the absence of magnetic fields.

Hence, depending on the external conditions, this *smart* composite material can be user-controlled to absorb different amounts of energy by modulating the magnetic field. Also, due to the fast response time of the FRFs, the energy absorption capacity can be rapidly switched to different levels in order to satisfy the application demands.

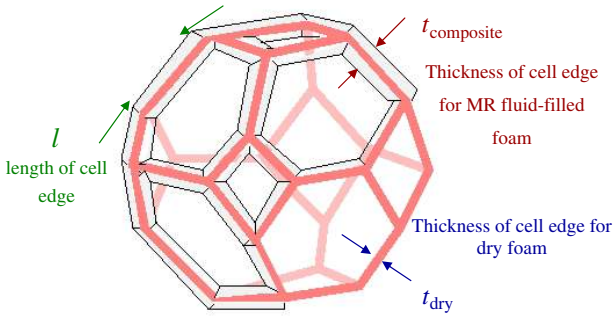

Figure 5. Schematic of a single tetrakaidecahedron cell of the MR fluid–foam composite showing a secondary layer of MRF on the solid foam cell edges.

We have also studied the behavior of the composite under the variation of control parameters besides the magnetic field strength, such as the imposed normal strain rate and the volume fraction of the MRF impregnating the reticulated foam. Varying the volume fraction of the MR fluid that is impregnated into the foam increases the thickness of the secondary layer of MR fluid that forms on the struts of the foam and hence increases the plateau stress. Also, more fluid needs to be squeezed out as the sample undergoes compression and hence the stress increases at lower densification strains as shown in figure 4(b). The energy absorbed by the MR fluid-impregnated foam can thus be modulated to satisfy specific requirements by controlling external parameters such as the applied magnetic field (B_{avg}) and the volume fraction (ϕ_{mrf}) of MR fluid.

4. 'Two-layer' model for the energy-absorbing composite

The energy absorption capacity of MR fluid-impregnated foam is a complex function of the control variables, B_{avg}, ϕ_{mrf}, the deformation rate, $\dot{\varepsilon}$ and geometric parameters describing the foam cells. Recently, a four-parameter viscoelastic–viscoplastic model was used to describe the cyclic loading of magnetorheological composites in dampers [19].

We develop a scaling model that considers the parametric variation of the plateau stress and can be used to optimize the amount of energy absorbed as a function of the different control parameters. This model, which we refer to as the 'two-layer' model, is based on the assumption that a fraction of the MR fluid impregnating the cellular solid covers the cell edges of the tetrakaidecahedron unit cell to form a uniform secondary fluid layer as illustrated in figure 5.

The portion of the impregnated MR fluid volume not forming the secondary layer has little effect on the plateau stress and only shifts the densification region to smaller strains in a manner similar to the case of a Newtonian fluid. The fraction (f) coating the cell walls is a single fitting parameter that depends on the type and geometry of cellular solid and the value of the field-off yield stress that inhibits fluid-film drainage. Our scaling model takes into account the changes in the effective elastic properties of the foam and also the geometric parameters; namely the thickness t, and length of the cell edge l. The thickness of the cell edge changes from t_{dry}

to $t_{\text{composite}}$ due to fluid impregnation while there is negligible change in length of the cell edge.

The plateau modulus (σ^*_{dry}) of open-cell elastomeric 'dry' foam (i.e. a foam with 0% v/v MR fluid) can be described as [1]

$$\sigma^*_{\text{dry}} \propto E_{\text{s}} \left(\frac{\rho^*}{\rho_{\text{s}}}\right)^2 \left[1 + \left(\frac{\rho^*}{\rho_{\text{s}}}\right)^{0.5}\right]^2, \tag{2}$$

where E_{s} is the elastic modulus of the solid material forming the cell struts and ρ^*/ρ_{s} is the relative density of the foam compared to the pure elastomeric solid.

The elastic modulus E_{s} of the solid changes as the amount of MR fluid forming the secondary layer on the cell edges varies with ϕ_{f}. This can be estimated by the 'rule of mixtures' for composites as follows:

$$E_{\text{composite}} = \frac{\phi_{\text{s}} E_{\text{s}} + \phi_{\text{f}} E_{\text{mrf}}}{\phi_{\text{s}} + \phi_{\text{f}}}$$
$$E_{\text{mrf}} \approx 3G_{\text{mrf}}(B), \qquad \phi_{\text{f}} = f\phi_{\text{mrf}}, \tag{3}$$

where ϕ_{s} is the solid volume fraction of the foam, ϕ_{f} is the fluid volume fraction in the cell edges, ϕ_{mrf} is the total volume fraction of the MRF impregnating the solid, E_{mrf} is the elastic modulus of the MR fluid and G_{mrf} is the shear modulus of the MR fluid as a function of the magnetic field strength which is determined by linear viscoelastic rheological measurements.

Although the elastic modulus of the composite decreases since $E_{\text{mrf}} < E_{\text{s}}$, there is an effective increase in the plateau modulus because the relative density of the composite (ρ^*/ρ_{s}) increases according to the following relationships:

$$\frac{\rho^*_{\text{dry}}}{\rho_{\text{s}}} \propto \left(\frac{t_{\text{dry}}}{l}\right)^2,$$
$$\frac{\rho^*_{\text{composite}}}{\rho_{\text{s}}} \propto \left(\frac{t_{\text{composite}}}{l}\right)^2, \tag{4}$$
$$\frac{(\pi/4)\left(t_{\text{composite}}\right)^2 l}{(\pi/4)\left(t_{\text{dry}}\right)^2 l} \approx \frac{\phi_{\text{f}} + \phi_{\text{s}}}{\phi_{\text{s}}},$$

where t_{dry} is the thickness of the dry foam cell and $t_{\text{composite}}$ is the thickness of the impregnated foam cell which can be computed from the volume fraction of the MR fluid, ϕ_{mrf}.

The increase in the plateau stress σ^* with respect to the dry or non-impregnated foam can thus be determined as a function of the magnetic field strength B, volume fraction of the MR fluid covering the cell edges ϕ_{f} and the plateau stress of the dry cellular solid σ^*_{dry} by the following expression:

$$\left(\frac{\sigma^*}{\sigma^*_{\text{dry}}}\right) = \left(\frac{E_{\text{composite}}}{E_{\text{s}}}\right)\left(\frac{\rho^*_{\text{composite}}}{\rho^*_{\text{dry}}}\right)^2 \times \left(\frac{1 + \sqrt{\left(\frac{\rho^*_{\text{composite}}}{\rho^*_{\text{dry}}}\right)\left(\frac{\rho^*_{\text{dry}}}{\rho_{\text{s}}}\right)}}{1 + \sqrt{\frac{\rho^*_{\text{dry}}}{\rho_{\text{s}}}}}\right)^2, \tag{5}$$

where

$$\frac{E_{\text{composite}}}{E_{\text{s}}} = \frac{1 + \left(\frac{\phi_{\text{f}}}{\phi_{\text{s}}}\right)\left(\frac{3G_{\text{mrf}}}{E_{\text{s}}}\right)}{1 + \frac{\phi_{\text{f}}}{\phi_{\text{s}}}}$$

and

$$\frac{\rho^*_{\text{composite}}}{\rho^*_{\text{dry}}} = 1 + \frac{\phi_{\text{f}}}{\phi_{\text{s}}}.$$

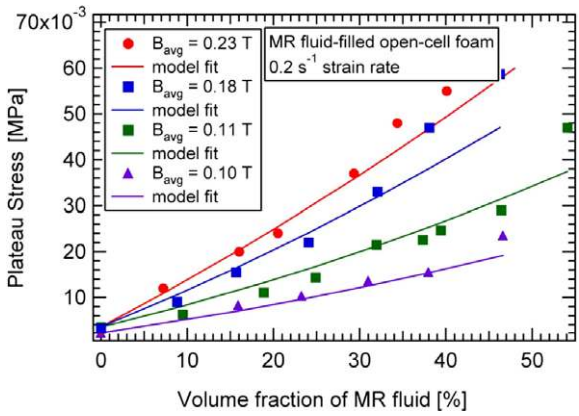

Figure 6. 'Two-layer' model fit to observed values of the plateau stress for MR fluid-filled open-cell foam samples.

The values denoted by the 'dry' subscript depend on the specific open-cell structure and solid foam material.

For collapse of data onto a single curve using equation (5), a fluid shift factor (a_{f}) is thus conveniently defined as follows:

$$a_{\text{f}} = \frac{\sigma^*}{\sigma^*_{\text{dry}}} = \zeta\left[1 + C_1(\zeta - 1)\right]\left[\frac{1 + \sqrt{C_2\zeta}}{1 + \sqrt{C_2}}\right] \tag{6}$$

where $\zeta = 1 + (\phi_{\text{f}}/\phi_{\text{s}})$, C_1 is a function of B and E_{s}, and C_2 depends on the foam structure. At low volume fractions of MR fluid, this plateau stress σ^* can be shown to vary almost linearly with the volume fraction (ϕ_{f}) as is also observed in figure 6.

The magnetic field gradient is also an important factor determining the stress–strain behavior of the MR fluid-filled foam sample since an additional force, called the ponderomotive magnetic force [20], is experienced when the sample is compressed either against or along the magnetic field gradient

$$f_v = \left(\frac{\chi}{\mu_0}\right) B_{\text{avg}} \frac{\text{d}B}{\text{d}z}, \tag{7}$$

where f_v is the ponderomotive force exerted per unit volume, χ is the magnetic susceptibility of the composite material, μ_0 is the magnetic permeability of free space and $\text{d}B/\text{d}z$ is the magnetic field gradient experienced by the sample.

The experimentally observed plateau stress (σ^*_{expt}) can then be expressed as a linear combination of this enhanced modulus and the ponderomotive force (f_v) as follows:

$$\sigma^*_{\text{expt}} = a_{\text{f}}\sigma^*_{\text{dry}} + f_v\left(\phi_{\text{mrf}} h\right), \tag{8}$$

where h is the height of the foam sample. Model fits to experimentally observed plateau stress values using the expressions for the shift factor (a_{f}) and ponderomotive magnetic force (f_v) for different volume fractions and magnetic fields are shown in figure 6.

Since the plateau region is much larger than the linear elastic region in reticulated polyurethane foam samples, it is possible to shift the stress–strain curves to form a single master curve at a chosen reference value of the volume fraction. Figure 7(a) illustrates this stress shifting for different volume fractions and at two different magnetic fields using the plateau

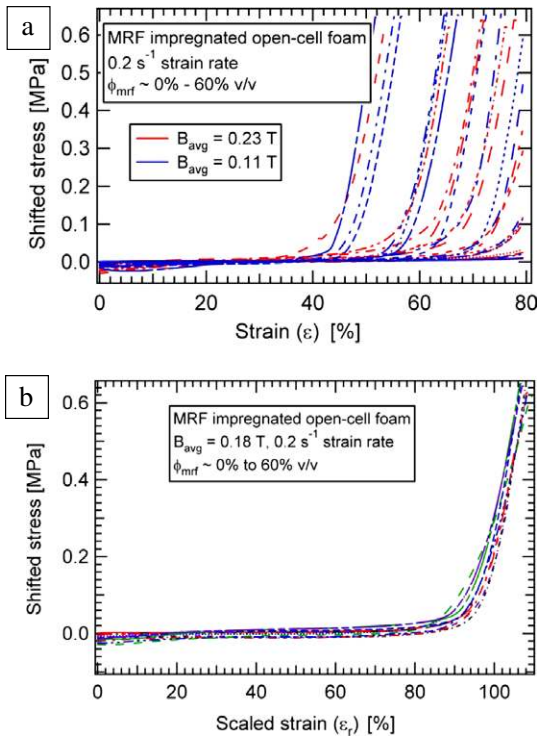

Figure 7. (a) 'Two-layer' model based stress shift to dry foam plateau stress ($\sigma^*_{\rm dry}$) for $0\% \leqslant \phi_{\rm mrf} \leqslant 60\%$ v/v MR fluid-impregnated foam. (b) Master curve for all control parameters obtained by using the 'two-layer' model based stress shift and strain scaling. The strain scaling accounts for the decrease in the free volume of the composite with increasing MR fluid volume fraction.

modulus for 'dry foam' (i.e. volume fraction $\phi_{\rm mrf} = 0\%$) as the reference condition. A single plateau stress curve is observed until the onset of the densification region, thus validating the model scalings described above.

The rescaling in the plateau stress with magnetic field, however, does not take into account the subsequent densification region, which is also a function of the volume fraction of the MR fluid. As the amount of incompressible fluid impregnating the cellular solid changes, the strain in the fluid–solid composite can also be scaled in accordance with the free volume available for compression in the following manner:

$$\varepsilon_{\rm r} = \frac{\varepsilon}{1 - (\phi_{\rm s} + \phi_{\rm f})} \tag{9}$$

where $\varepsilon_{\rm r}$ is the scaled or 'reduced' strain, $\phi_{\rm s}$ is the solid volume fraction and $\phi_{\rm f}$ is the MR fluid volume fraction in the composite. The subsequent master curve of 'reduced strain' against the 'shifted stress' for different volume fractions of MR fluid impregnating the foam at a reference field strength of 0.18 T is illustrated in figure 7(b).

The 'two-layer' scaling model thus enables the construction of a master curve, which collapses all of the observed experimental data. This master curve can now be used to determine the mechanical properties of MR fluid-impregnated foams for different values of B, $\phi_{\rm mrf}$ and also provides an effective tool for optimizing the energy absorption capacity in tune with specific application requirements.

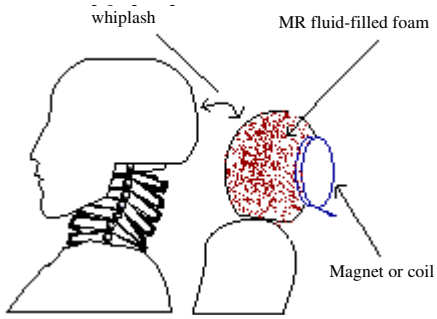

Figure 8. Illustration of a MR fluid-impregnated headrest in an automobile to satisfy the 'neck injury criterion' ($\rm NIC = 0.2a_{rel} + (v_{rel})^2 < 15\ m^2\ s^{-2}$) [22] and prevent whiplash-associated disorders (WAD).

5. Application potential and design considerations

5.1. Application potential for the adaptive material

A number of application areas from ballistic armor to automotive components can be envisaged for this *smart material*. In the automotive industry, energy management is a big concern as new incoming Federal and European community legislations (FMVSS 201/202, EURO NCAP, EEVC WG 17) [7] introduce stringent impact protection requirements. Automobile parts would need to provide protection for two distinctly different sizes (adult and child) of pedestrian and passenger, which present many 'conflict areas' with different stiffness requirements under various conditions. A possible solution to this *conflict of stiffness* problem involves constructing interior components of the vehicle, such as the headrest, A/B/C pillar trims, head-liners, knee and side impact foam parts, with an adaptive material so that the different energy absorption criteria under varying impact conditions and constraints of interior/exterior space and design can be satisfied [21].

This *adaptive composite* could also be extremely beneficial in automotive injury prevention. NHTSA estimated that there were 805 851 occupants with whiplash injuries alone, annually between 1988 and 1996 in the United States resulting in a total annual cost of $5.2 billion. Whiplash associated disorders are influenced mainly by seat and head-restraint properties and their positions with respect to the head and torso. The number and extent of injuries can be reduced by maximizing the amount of energy absorption, by minimizing the occupant acceleration or by reducing the relative movement between the head and the torso [22]. A soft compliant headrest, though comfortable, would imply a high risk for whiplash injury because of large head–neck relative movement. A field-responsive fluid-impregnated headrest would allow the same headrest to be soft and compliant under normal driving conditions but then can be switched into a high impact energy-absorbing stiff material during a crash, as illustrated in figure 8.

However, many issues need to be addressed before successful commercialization of these energy managing structures. The heat transfer of the energy dissipated during compression and the power consumed for magnetic field generation are important concerns that need to be studied in detail. Another important consideration for all these

applications is the generation of a strong, rapidly modifiable distributed magnetic field for active energy absorption. Various embodiments of energy management structures, depending on the application constraints, such as by using a permanent magnet or a field coil are described elsewhere [21]. Impact applications, such as an automotive energy-absorbing headrest, require a magnetic field only during the time of impact (100–300 ms) which can be exploited by using a capacitor discharge to rapidly generate a strong distributed magnetic field with minimum power consumption.

5.2. Smart composite based automotive headrest: design and impact testing

The energy absorbed by the MR fluid-impregnated headrest (W) can be described as a function of a number of parameters such as the initial impact energy, foam structural and mechanical properties and dimensions of the head model. The general functional relationship is expected to be of the form

$$W = F\left(E_i, d, h, \phi_f, B_{avg}, \frac{\rho^*}{\rho_s}\right), \tag{10}$$

where E_i is the kinetic energy of the head (or model) before impact, d is the characteristic diameter of the impacting object, h is the thickness of the foam, ϕ_f is the volume fraction of the fluid impregnating the foam, B_{avg} is the average external magnetic field applied and ρ^*/ρ_s is the relative density of the reticulated foam. The parameters characterizing the MR fluid-impregnated foam are, however, interdependent and can be expressed in terms of the plateau stress (σ^*) as described in equation (6). Dimensional analysis for the amount of energy absorbed then gives

$$\frac{W}{E_i} = f^n\left(\frac{d}{h}, \frac{\sigma^*}{\sigma^*_{dry}}\right), \tag{11}$$

where W/E_i is the fraction of impact energy absorbed or, in related terms, the coefficient of restitution $\varepsilon = (1 - W/E_i)$ which is the unabsorbed fraction of impact energy and σ^*/σ^*_{dry} is the shift factor given by equation (6) which characterizes the material properties of the fluid-impregnated foam.

A 'drop-ball' test apparatus has been custom-built in our laboratory for simulating headrest-design impacts. The technique consists of dropping a guided ball from a variable height through a guide tube onto the middle of a specimen and measuring the velocity, acceleration and the amount of energy absorbed. A clear acrylic tube is used as the guide rail and sleeve for the sample in order to allow easy visualization. A high-speed digital video camera (Phantom v5.0, Vision Research Inc.) connected to a computer is used to record the impact trajectory of the ball on the sample at 1900 frames per second. For simulating impact on a scaled headrest, an average human head that weighs around 4500–5000 g with a characteristic diameter of 16.5 cm [23] crashing into a car headrest is scaled down to a 1.27 mm aluminum ball weighing 3 g impacting a MR fluid-filled cylindrical sample of 3.8 cm diameter and 1.9 cm height. The ball is dropped from an average height of 150 cm and impacts at an average velocity of 5.3 m s^{-1} (~20 km/h), which is the maximum velocity used in automobile rear-end crash design [23]. This scaling

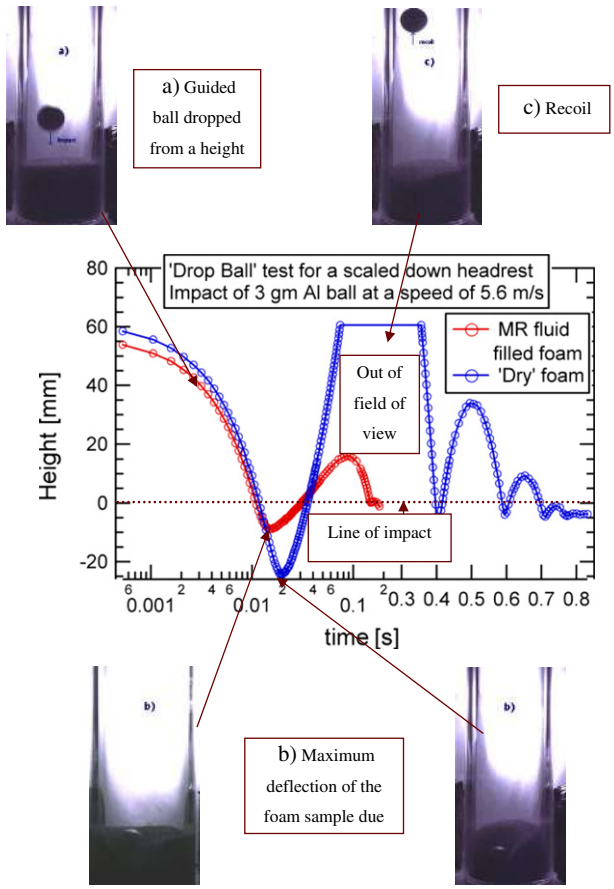

Figure 9. Real-time impact testing of a geometrically scaled adult headform onto a car headrest using a 'drop-ball' test apparatus. An average magnetic field strength ($B_{avg} = 0.15$ T) is applied to the foam sample impregnated with $\phi_{mrf} = 35\%$ v/v.

ensures a geometric and kinematic similarity to the actual impact scenario. Also, the initial impact energy per unit volume (E_i/V) is maintained the same for dynamic similarity.

The trajectory of the ball motion during a simulated impact is plotted in figure 9 with corresponding image captures at maximum deflection and recoil positions. Whilst the MR fluid-filled foam (video1(b) available at stacks.iop.org/SMS/16/106) shows only 30% compression with a rebound velocity of 0.5 m s^{-1}, the 'dry' foam sample (video1(a) available at stacks.iop.org/SMS/16/106) 'bottoms out' with nearly 100% compression on impact and the ball rebounds at 1.72 m s^{-1}. The coefficient of restitution for the MR fluid-filled foam ($\varepsilon = 0.1$) is much less compared to the unfilled foam ($\varepsilon = 0.3$) despite having less than one-third the total compression of the unfilled foam. The maximum compression of the foam sample corresponds to the total relative movement between the neck pivot point and the back of the head in an actual crash and its reduction is highly beneficial. The rebound velocity relates to the forward rebound of the passenger onto the seat belt in crash conditions and hence is also a vital consideration for whiplash injury minimization [22, 23]. These comparative tests demonstrate in principle the effectiveness of using a headrest impregnated with a field-responsive fluid for protection of passengers in a rear-end impact.

6. Conclusions

To summarize, we have prepared stable, inexpensive MR fluids and have shown that they can be used to modulate the stiffness and energy absorption capacity of cellular solids. MR fluid-impregnated reticulated foams have energy absorption capacities controlled by moderate magnetic fields varying by factors of 1- to 50-fold above that of the corresponding field-off state. A scaling model has been proposed that enables experimental data for different control parameters to be collapsed onto a single master curve.

Shear-thickening fluids, which also belong to the broad class of field-responsive fluids and respond when acted upon by a stress field, can also be impregnated into reticulated foams to provide a passive or potentially an active mechanism for adaptive energy absorption. These fluids are currently being characterized and modeled for future use in adaptive energy management structures. Thus, a 'novel' class of conformable field-responsive fluid-based composites has been conceptualized, modeled and tested so that they can be used for wide-ranging rapidly-switchable energy-absorbing applications. These adaptive or tunable 'smart' materials should also prove beneficial in solving stiffness conflicts and crash management concerns in the automotive industry.

Acknowledgments

The authors would like to acknowledge the financial support received for this project from CC++ (Car Consortium) at the MIT Media labs and the Institute of Soldier Nanotechnologies (ISN).

References

[1] Gibson L J and Ashby M F 1997 *Cellular Solids: Structure and Properties* (Cambridge: Cambridge University Press)
[2] Cheeseman B A and Bogetti T A 2003 Ballistic impact into fabrics and compliant composite laminates *Comput. Struct.* **61** 161–73
[3] Gooding E 1999 Adaptive, energy absorbing structure *US Patent Specification* 5915819
[4] Kanianthra J N 1996 Side impact energy absorber *US Patent Specification* 5564535
[5] Courtney W A and Oyadiji S O 2001 Preliminary investigations into the mechanical properties of a novel shock absorbing elastomeric composite *J. Mater. Proc. Technol.* **119** 379–86
[6] Holnicki-Szulc J, Pawlowski P and Wiklo M 2003 High-performance impact absorbing materials—the concept, design tools and applications *Smart Mater. Struct.* **12** 461–7
[7] Ullrich M 2003 Caught between the constraints of interior design and safety *IVehE* 26–7
[8] Hayes W C, Robinovitch S N and McMahon T A 1996 Bone fracture prevention method *US Patent Specification* 5545128 A
[9] Larson R G 1999 *The Structure and Rheology of Complex Fluids* (New York: Oxford University Press)
[10] Barnes H A 1989 Shear-thickening (dilatancy) in suspensions of nonaggregating solid particles dispersed in newtonian liquids *J. Rheol.* **33** 329–66
[11] Ginder J M 1996 Rheology controlled by magnetic fields *Encyclopedia of Applied Physics* vol 16 (New York: VCH) p 487
[12] Klingenberg D J 2001 Magnetorheology: applications and challenges *AIChE J.* **47** 246–9
[13] Barnes H A 1999 The yield stress—a review or '$\pi\alpha\nu\tau\alpha\ \rho\varepsilon\iota$'—everything flows? *J. Non-Newton. Fluid Mech.* **81** 133–78
[14] Genc S and Phule P P 2002 Rheological properties of magnetorheological fluids *Smart Mater. Struct.* **11** 140–6
[15] Deshmukh S S and McKinley G H 2004 Rheological behavior of magnetorheological suspensions under shear, creep and large amplitude oscillatory shear (LAOS) flow *Proc. XIVth Int. Congr. on Rheology (Seoul, Korea, Aug. 2004)*
[16] Carlson J D and Jolly M R 2000 MR fluid, foam and elastomer devices *Mechatronics* **10** 555–69
[17] Chrzan M J and Carlson J D 2001 MR fluid sponge devices and their use in vibration control of washing machines *Proc. 8th Symp. on Smart Structures and Materials (Newport Beach, CA)*
[18] Jolly M R, Bender J W and Carlson J D 1999 Properties and applications of commercial magnetorheological fluids *J. Intell. Mater. Syst. Struct.* **10** 5–13
[19] Kaleta J, Lewandowski D and Zajac P 2005 Experimental identification of magnetorheological composites and elastomers *Mater. Struct. Micromechanics of Fracture, Mater. Sci. Forum* **482** 403–7
[20] Uetake H, Hiroto N, Nakagawa J, Ikezoe Y and Kitazawa K 2000 Thermal convection control by gradient magnetic field *J. Appl. Phys.* **87** 6310
[21] Deshmukh S S and McKinley G H 2002 Fluid-filled cellular solids for controlled energy absorption *US Patent Appl. No.* 10/378 129
[22] Svensson M Y, Lovsund P, Haland Y and Larsson S 1996 The influence of seat-back and head-restraint properties on the head-neck motion during rear-impact *Accid. Anal. Prev.* **28** 221–7
[23] Jakobsson L, Lundell B, Norin H and Isaksson-Hellman I 2000 WHIPS–volvo's whiplash protection study *Accid. Anal. Prev.* **32** 307–19